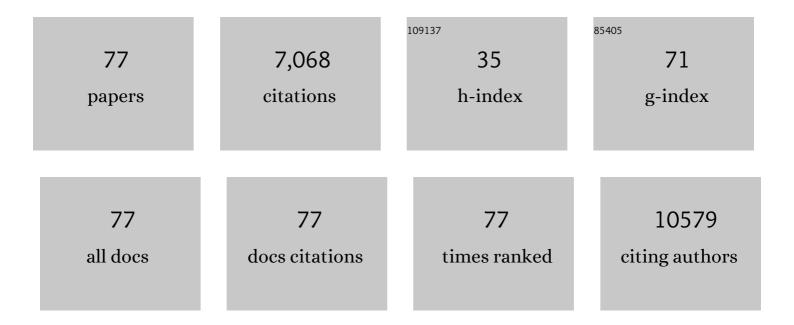
List of Publications by Year in descending order

Source: https://exaly.com/author-pdf/3840730/publications.pdf

Version: 2024-02-01



VANROLI

#	Article	IF	CITATIONS
1	Interface engineering of Ta3N5 thin film photoanode for highly efficient photoelectrochemical water splitting. Nature Communications, 2022, 13, 729.	5.8	99
2	Tuning the Selectivity of Liquid Products of CO ₂ RR by Cu–Ag Alloying. ACS Applied Materials & Interfaces, 2022, 14, 11567-11574.	4.0	44
3	Coevaporation of Doped Inorganic Carrierâ€Selective Layers for Highâ€Performance Inverted Planar Perovskite Solar Cells. Solar Rrl, 2022, 6, .	3.1	4
4	Direct synthesis of BaTaO2N nanoparticle film on a conductive substrate for photoelectrochemical water splitting. Journal of Catalysis, 2022, 411, 109-115.	3.1	5
5	Tailoring the Crystallographic Orientation of a Sb ₂ S ₃ Thin Film for Efficient Photoelectrochemical Water Reduction. ACS Catalysis, 2022, 12, 8175-8184.	5.5	20
6	Selfâ€Assembly of Colloidal Nanoparticles into Wellâ€Ordered Centimeterâ€Long Rods via Crack Engineering. Advanced Materials Interfaces, 2021, 8, 2000222.	1.9	6
7	Metastable Ta ₂ N ₃ with highly tunable electrical conductivity <i>via</i> oxygen incorporation. Materials Horizons, 2021, 8, 1744-1755.	6.4	6
8	Polyacetylene derivatives in perovskite solar cells: from defect passivation to moisture endurance. Journal of Materials Chemistry A, 2021, 9, 13220-13230.	5.2	15
9	Atomic Layer Deposition for the Photoelectrochemical Applications. Advanced Materials Interfaces, 2021, 8, 2002100.	1.9	17
10	Revealing the Aging Effect of Metal-Oleate Precursors on the Preparation of Highly Luminescent CsPbBr ₃ Nanoplatelets. Journal of Physical Chemistry Letters, 2021, 12, 2668-2675.	2.1	15
11	Perovskite single crystals: Synthesis, properties, and applications. Journal of Electronic Science and Technology, 2021, 19, 100081.	2.0	41
12	Improving photoelectrochemical water oxidation activity of BiFeO3 photoanode via surface passivation. Applied Physics Letters, 2021, 119, 013903.	1.5	7
13	A rational design strategy for red thermally activated delay fluorescence emitter employing 2,1,3-benzothiadiazole skeleton with asymmetric structure. Dyes and Pigments, 2021, 196, 109781.	2.0	10
14	A self-healing catalyst for electrocatalytic and photoelectrochemical oxygen evolution in highly alkaline conditions. Nature Communications, 2021, 12, 5980.	5.8	88
15	lonic liquid-induced <i>in situ</i> deposition of perovskite quantum dot films with a photoluminescence quantum yield of over 85%. Nanoscale, 2021, 13, 20067-20077.	2.8	3
16	All-Inorganic Perovskite Solar Cells: Energetics, Key Challenges, and Strategies toward Commercialization. ACS Energy Letters, 2020, 5, 290-320.	8.8	183
17	Band structure engineering and defect control of Ta3N5 for efficient photoelectrochemical water oxidation. Nature Catalysis, 2020, 3, 932-940.	16.1	211
18	Earth-abundant Cu-based metal oxide photocathodes for photoelectrochemical water splitting. Energy and Environmental Science, 2020, 13, 3269-3306.	15.6	141

#	Article	IF	CITATIONS
19	Synthesis, crystal structure, aggregation-induced emission (AIE) and electroluminescence properties of a novel emitting material based on pyrrolo[3,2- <i>b</i>]pyrrole. Journal of Materials Chemistry C, 2020, 8, 14208-14218.	2.7	14
20	Identifying Performance-Limiting Deep Traps in Ta ₃ N ₅ for Solar Water Splitting. ACS Catalysis, 2020, 10, 10316-10324.	5.5	68
21	Tuning Hole Accumulation of Metal Oxides Promotes the Oxygen Evolution Rate. ACS Catalysis, 2020, 10, 10427-10435.	5.5	10
22	Strongly Enhanced Photoluminescence and Photoconductivity in Erbium-Doped MAPbBr ₃ Single Crystals. Journal of Physical Chemistry C, 2020, 124, 8992-8998.	1.5	26
23	Fe-Based Electrocatalysts for Oxygen Evolution Reaction: Progress and Perspectives. ACS Catalysis, 2020, 10, 4019-4047.	5.5	379
24	Hybrid microbial photoelectrochemical system reduces CO2 to CH4 with 1.28% solar energy conversion efficiency. Chemical Engineering Journal, 2020, 390, 124530.	6.6	44
25	An ultrathin MoSe ₂ photodetector with near-perfect absorption. Nanotechnology, 2020, 31, 225201.	1.3	29
26	Tailored NiFe Catalyst on Silicon Photoanode for Efficient Photoelectrochemical Water Oxidation. Journal of Physical Chemistry C, 2020, 124, 2844-2850.	1.5	19
27	Large organic cation incorporation induces vertical orientation growth of Sn-based perovskites for high efficiency solar cells. Chemical Engineering Journal, 2020, 402, 125133.	6.6	25
28	Large-Area Organic-Free Perovskite Solar Cells with High Thermal Stability. Journal of Physical Chemistry Letters, 2019, 10, 6382-6388.	2.1	46
29	Enhanced thermal stability of electron transport layer-free perovskite solar cells via interface strain releasing. Journal of Power Sources, 2019, 439, 227091.	4.0	21
30	Defect-Rich NiCeO _{<i>x</i>} Electrocatalyst with Ultrahigh Stability and Low Overpotential for Water Oxidation. ACS Catalysis, 2019, 9, 1605-1611.	5.5	113
31	Steering the crystallization of perovskites for high-performance solar cells in ambient air. Journal of Materials Chemistry A, 2019, 7, 12166-12175.	5.2	65
32	The rational design of hierarchical MoS ₂ nanosheet hollow spheres sandwiched between carbon and TiO ₂ @graphite as an improved anode for lithium-ion batteries. Nanoscale Advances, 2019, 1, 1957-1964.	2.2	4
33	High Photovoltage Inverted Planar Heterojunction Perovskite Solar Cells with All-Inorganic Selective Contact Layers. ACS Applied Materials & Interfaces, 2019, 11, 46894-46901.	4.0	20
34	Efficient photoelectrochemical water oxidation enabled by an amorphous metal oxide-catalyzed graphene/silicon heterojunction photoanode. Sustainable Energy and Fuels, 2018, 2, 663-672.	2.5	25
35	Hierarchical MoS2/Ni3S2 core-shell nanofibers for highly efficient and stable overall-water-splitting in alkaline media. Materials Today Energy, 2018, 10, 214-221.	2.5	16
36	Engineering graphene and TMDs based van der Waals heterostructures for photovoltaic and photoelectrochemical solar energy conversion. Chemical Society Reviews, 2018, 47, 4981-5037.	18.7	344

#	Article	IF	CITATIONS
37	Hybrid solar-to-methane conversion system with a Faradaic efficiency of up to 96%. Nano Energy, 2018, 53, 232-239.	8.2	76
38	Perfect invisibility concentrator with simplified material parameters. Frontiers of Physics, 2018, 13, 1.	2.4	11
39	Size-dependent longitudinal plasmon resonance wavelength and extraordinary scattering properties of Au nanobipyramids. Nanotechnology, 2018, 29, 355402.	1.3	24
40	Determining Atomic-Scale Structure and Composition of Organo-Lead Halide Perovskites by Combining High-Resolution X-ray Absorption Spectroscopy and First-Principles Calculations. ACS Energy Letters, 2017, 2, 1183-1189.	8.8	23
41	Promotion on Acetone Sensing of Single SnO2 Nanobelt by Eu Doping. Nanoscale Research Letters, 2017, 12, 405.	3.1	25
42	Fast Growth of Highly Ordered TiO2 Nanotube Arrays on Si Substrate under High-Field Anodization. Nano-Micro Letters, 2017, 9, 13.	14.4	10
43	Low Pressure Vapor-assisted Solution Process for Tunable Band Gap Pinhole-free Methylammonium Lead Halide Perovskite Films. Journal of Visualized Experiments, 2017, , .	0.2	0
44	Scalable Low-Band-Gap Sb ₂ Se ₃ Thin-Film Photocathodes for Efficient Visible–Near-Infrared Solar Hydrogen Evolution. ACS Nano, 2017, 11, 12753-12763.	7.3	127
45	Solution-processed CuSbS2 thin film: A promising earth-abundant photocathode for efficient visible-light-driven hydrogen evolution. Nano Energy, 2016, 28, 135-142.	8.2	70
46	Defective TiO2 with high photoconductive gain for efficient and stable planar heterojunction perovskite solar cells. Nature Communications, 2016, 7, 12446.	5.8	139
47	Facet-dependent photovoltaic efficiency variations in single grains of hybrid halideÂperovskite. Nature Energy, 2016, 1, .	19.8	308
48	Scalable water splitting on particulate photocatalyst sheets with a solar-to-hydrogen energy conversion efficiency exceeding 1%. Nature Materials, 2016, 15, 611-615.	13.3	1,311
49	High Photoluminescence Quantum Yield in Band Gap Tunable Bromide Containing Mixed Halide Perovskites. Nano Letters, 2016, 16, 800-806.	4.5	269
50	Z-scheme water splitting using particulate semiconductors immobilized onto metal layers for efficient electron relay. Journal of Catalysis, 2015, 328, 308-315.	3.1	119
51	Fabrication of Planar Heterojunction Perovskite Solar Cells by Controlled Low-Pressure Vapor Annealing. Journal of Physical Chemistry Letters, 2015, 6, 493-499.	2.1	112
52	A Novel Method to Synthesize Highly Photoactive Cu ₂ O Microcrystalline Films for Use in Photoelectrochemical Cells. ACS Applied Materials & Interfaces, 2014, 6, 480-486.	4.0	107
53	Fabrication of highly ordered Ta ₂ O ₅ and Ta ₃ N ₅ nanorod arrays by nanoimprinting and through-mask anodization. Nanotechnology, 2014, 25, 014013.	1.3	14
54	Wafer-Scale Fabrication of Self-Catalyzed 1.7 eV GaAsP Core–Shell Nanowire Photocathode on Silicon Substrates. Nano Letters, 2014, 14, 2013-2018.	4.5	58

#	Article	IF	CITATIONS
55	Core/Shell Structured La- and Rh-Codoped SrTiO ₃ as a Hydrogen Evolution Photocatalyst in Z-Scheme Overall Water Splitting under Visible Light Irradiation. Chemistry of Materials, 2014, 26, 4144-4150.	3.2	242
56	Cobalt phosphate-modified barium-doped tantalum nitride nanorod photoanode with 1.5% solar energy conversion efficiency. Nature Communications, 2013, 4, 2566.	5.8	306
57	Vertically Aligned Ta ₃ N ₅ Nanorod Arrays for Solarâ€Driven Photoelectrochemical Water Splitting. Advanced Materials, 2013, 25, 125-131.	11.1	363
58	Photoelectrodes: Vertically Aligned Ta ₃ N ₅ Nanorod Arrays for Solarâ€Driven Photoelectrochemical Water Splitting (Adv. Mater. 1/2013). Advanced Materials, 2013, 25, 152-152.	11.1	4
59	ZnO–ZnGa ₂ O ₄ core–shell nanowire array for stable photoelectrochemical water splitting. Nanoscale, 2012, 4, 1509-1514.	2.8	77
60	Vertically aligned ZnO–ZnGa2O4 core–shell nanowires: from synthesis to optical properties. Journal of Nanoparticle Research, 2012, 14, 1.	0.8	12
61	Stability of hydrogen incorporated in ZnO nanowires by plasma treatment. Nanotechnology, 2011, 22, 435703.	1.3	13
62	Bridging wide bandgap nanowires for ultraviolet light detection. , 2011, , .		0
63	Morphological evolution of large-scale vertically aligned ZnO nanowires and their photoluminescence properties by hydrogen plasma treatment. Materials Research Society Symposia Proceedings, 2011, 1302, 8101.	0.1	0
64	Efficient Assembly of Bridged <i>β</i> â€Ga ₂ O ₃ Nanowires for Solarâ€Blind Photodetection. Advanced Functional Materials, 2010, 20, 3972-3978.	7.8	292
65	Progress Toward Nanowire Device Assembly Technology. , 2010, , .		4
66	Bascule nanobridges self-assembled with ZnO nanowires as double Schottky barrier UV switches. Nanotechnology, 2010, 21, 295502.	1.3	38
67	Enhancement of Gas Response of ZnO Micro-nano Structured Films through O2 Plasma Treatment. IEEJ Transactions on Sensors and Micromachines, 2009, 129, 307-311.	0.0	0
68	Competitive surface effects of oxygen and water on UV photoresponse of ZnO nanowires. Applied Physics Letters, 2009, 94, .	1.5	218
69	High-performance UV detector made of ultra-long ZnO bridging nanowires. Nanotechnology, 2009, 20, 045501.	1.3	192
70	Effect of hydrogen plasma treatment on the luminescence and photoconductive properties of ZnO nanowires. Materials Research Society Symposia Proceedings, 2009, 1206, 130301.	0.1	3
71	Fabrication of Hierarchical ZnO Architectures and Their Superhydrophobic Surfaces with Strong Adhesive Force. Inorganic Chemistry, 2008, 47, 3140-3143.	1.9	79
72	Fabrication of ZnO Bridging Nanowire Device by a Single-Step Chemical Vapor Deposition Method. Materials Research Society Symposia Proceedings, 2008, 1144, 1.	0.1	1

#	Article	IF	CITATIONS
73	Self-assembly of versatile tubular-like In2O3nanostructures. Nanotechnology, 2007, 18, 465605.	1.3	17
74	High-speed growth and photoluminescence of porous anodic alumina films with controllable interpore distances over a large range. Applied Physics Letters, 2007, 91, .	1.5	59
75	Tip-like anodic alumina. Nanotechnology, 2007, 18, 215304.	1.3	8
76	Fabrication of highly ordered nanoporous alumina films by stable high-field anodization. Nanotechnology, 2006, 17, 5101-5105.	1.3	153
77	Wide-bandgap nanowires for UV-light detection. SPIE Newsroom, 0, , .	0.1	1